Pharmacological Research 125 (2017) 122–131

Contents lists available at ScienceDirect

Pharmacological Research

journal homepage: www.elsevier.com/locate/yphrs

Original article

Alisporivir rescues defective mitochondrial respiration in Duchenne muscular dystrophy

Marco Schiavone[a,1], Alessandra Zulian[a,1], Sara Menazza[a], Valeria Petronilli[a], Francesco Argenton[b], Luciano Merlini[c], Patrizia Sabatelli[d,e], Paolo Bernardi[a,*]

[a] Department of Biomedical Sciences and CNR Neuroscience Institute, University of Padova, Padova, Italy
[b] Department of Biology, University of Padova, Padova, Italy
[c] Department of Biomedical and Neuromotor Sciences, University of Bologna, Bologna, Italy
[d] Institute of Molecular Genetics, CNR, Bologna, Italy
[e] SC Laboratory of Musculoskeletal Cell Biology, IOR-IRCCS, Bologna, Italy

ARTICLE INFO

Article history:
Received 26 July 2017
Received in revised form 5 September 2017
Accepted 5 September 2017
Available online 9 September 2017

Keywords:
Duchenne muscular dystrophy
Mitochondria
Respiration
Cyclophilin
Permeability transition

ABSTRACT

Duchenne muscular dystrophy (DMD) is a severe muscle disease of known etiology without effective, or generally applicable therapy. Mitochondria are affected by the disease in animal models but whether mitochondrial dysfunction is part of the pathogenesis in patients remains unclear. We show that primary cultures obtained from muscle biopsies of DMD patients display a decrease of the respiratory reserve, a consequence of inappropriate opening of the permeability transition pore (PTP). Treatment with the cyclophilin inhibitor alisporivir – a cyclosporin A derivative that desensitizes the PTP but does not inhibit calcineurin – largely restored the maximal respiratory capacity without affecting basal oxygen consumption in cells from patients, thus reinstating a normal respiratory reserve. Treatment with alisporivir, but not with cyclosporin A, led to a substantial recovery of respiratory function matching improved muscle ultrastructure and survival of *sapje* zebrafish, a severe model of DMD where muscle defects are close to those of DMD patients. Alisporivir was generally well tolerated in HCV patients and could be used for the treatment of DMD.

1. Introduction

Duchenne muscular dystrophy (DMD) is a severe disease caused by defects of the gene encoding for dystrophin, a key component of muscle [1,2]. Dystrophin interacts with several partners to form the dystrophin-associated dystroglycan complex [3,4], which provides a link between the cytoskeleton and the sarcolemma [5,6]. This link further extends to the extracellular matrix through the interactions of dystroglycan and sarcoglycan with a variety of proteins including agrin, biglycan and their ligands laminin and collagen VI [4]. Dystrophin thus plays a key role in the stability of the sarcolemma in the face of muscle contraction, and it is not surprising that muscular dystrophies can arise from defects in the genes encoding for each component of this connecting system [4].

Mechanical stress is an inevitable consequence of muscle activity. Lack of dystrophin sensitizes muscle to damage followed by fiber death, inflammation and repair resulting in fibrosis, which eventually predominates over regeneration [4]. Increased permeability of the sarcolemma to Ca^{2+} is an early event that can lead to cell death [7], yet it is obvious that the defect is initially compensated [4]. Understanding the molecular bases of this compensation – and the reasons underlying their failure – can have a profound influence on rational therapeutic approaches downstream of the genetic lesion [4].

Animal models indicate that increased Ca^{2+} flux is a pathogenic event *per se* and that muscle disease occurs irrespective of the primary Ca^{2+} transport pathway that has been affected [7,8]. Early work had shown that total Ca^{2+} is increased in DMD fibers [9–11], and that the increase of cytosolic [Ca^{2+}] leads to protein degradation [12,13]. Deregulation of Ca^{2+} homeostasis does not necessarily mean that resting cytosolic [Ca^{2+}] is stably higher than normal

Abbreviations: alisporivir, *N*-methyl-D-alanine-3-*N*-ethyl-valine-4-cyclosporin; CyP, cyclophilin; Cs, cyclosporin; DMD, Duchenne muscular dystrophy; DMEM, Dulbecco's modified Eagle's medium; dpf, days post fertilization; FCCP, carbonylcyanide-*p*-trifluoromethoxyphenyl hydrazone; hpf, hours post fertilization; MTJ, myotendinous junction; NIM811, *N*-methyl-isoleucine-4-cyclosporin; OCR, oxygen consumption rate; PTP, permeability transition pore; TMRM, tetramethylrhodamine methyl ester.

* Corresponding author at: Department of Biomedical Sciences, University of Padova, Via Ugo Bassi 58/B, I-35131 Padova, Italy.
E-mail address: bernardi@bio.unipd.it (P. Bernardi).

[1] Equal contribution.

http://dx.doi.org/10.1016/j.phrs.2017.09.001

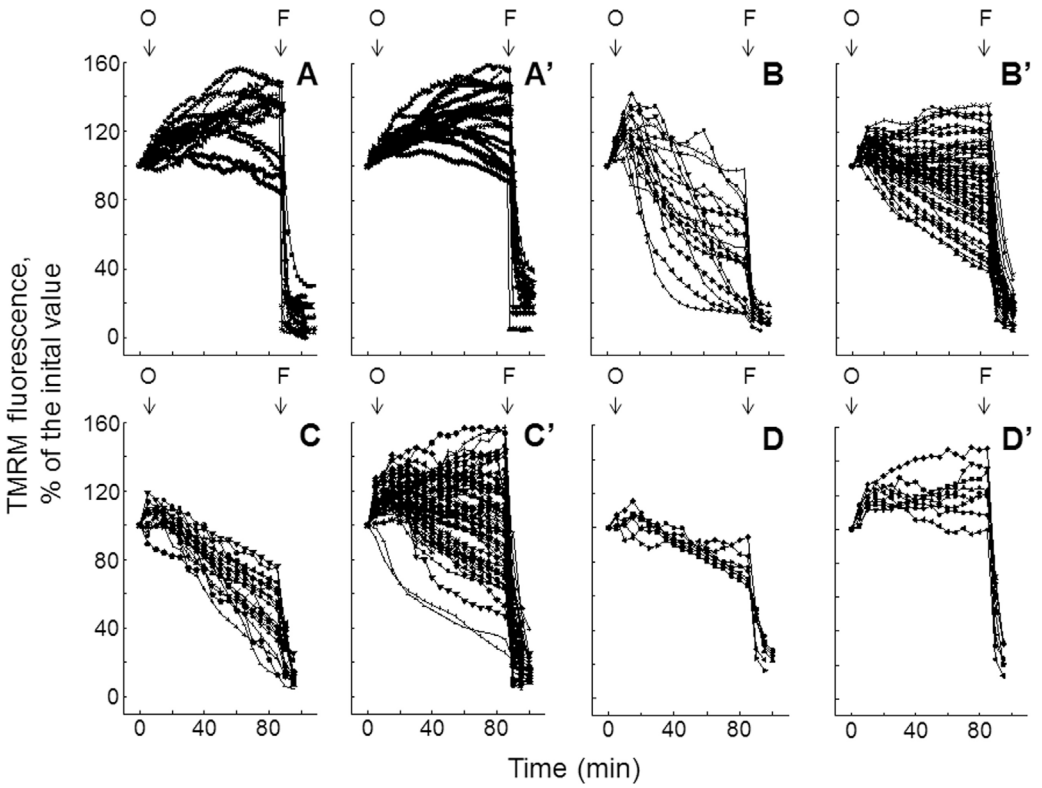

Fig. 1. Effect of alisporivir on oligomycin-induced mitochondrial depolarization in primary muscle cell cultures. Mitochondrial membrane potential was monitored based on TMRM fluorescence changes in primary cultures established from muscle biopsies of one healthy donor (**A, A'**) or of DMD patient 1 (**B, B'**), 2 (**C,C'**) and 3 (**D, D'**) and incubated in serum free-DMEM supplemented with 10 nM TMRM. Fluorescence was monitored over mitochondria-rich regions and acquired every 2 min for healthy donors and every 5 min for DMD patients. Where indicated by arrows, 6 μM oligomycin (O) and 4 μM FCCP (F) were added in the absence (**A–D**) or presence (**A'–D'**) of 1.6 μM alisporivir. Each line reports fluorescence of one individual cell.

[14,15]. It appears likely that increased Ca^{2+} flux at the sarcolemma [16,17] is initially compensated by intracellular organelles, and that a stable cytosolic [Ca^{2+}] rise may be a late event that triggers hypercontracture and activation of proteolytic enzymes, setting the point of no return and fiber death as first proposed 40 years ago [18]. This Ca^{2+}-dependent mitochondrial dysfunction may be due to opening of the mitochondrial permeability transition pore (PTP) [8].

The PTP is an inner membrane channel implicated in a variety of degenerative diseases. Its opening requires matrix Ca^{2+} – a key permissive factor – and is favored by oxidants, while it is counteracted by reducing agents, adenine nucleotides and Mg^{2+} [8]. The PTP appears to originate from a conformational change of the F_1F_O ATP synthase through a Ca^{2+}-dependent mechanism that is the matter of active investigation [19]. A key regulator of the PTP in vertebrates is matrix cyclophilin (CyP) D, whose inhibition is the basis for the PTP desensitizing effects of cyclosporin (Cs) A and of its non-immunosuppressive derivatives *N*-methyl-isoleucine-4-cyclosporin (NIM811) [20] and *N*-methyl-D-alanine-3-*N*-ethyl-valine-4-cyclosporin (alisporivir or Debio025, formerly Unil025) [21]. A role of the PTP in the pathogenesis of muscular dystrophy has been documented particularly for collagen VI diseases. Treatment with CsA and alisporivir was extremely effective in the *Col6a1*$^{-/-}$ myopathic mouse lacking collagen VI [22,23] and in cultured cells form patients [23,24], and NIM811 was superior to CsA in a severe zebrafish model of the disease [25,26]. Is PTP-dependent mitochondrial dysfunction also relevant to DMD? Treatment with alisporivir had beneficial effects in the *mdx* mouse [27,28], where it was more active than prednisone [29]. The limit of these studies is that the *mdx* mouse has a very mild disease and it remains unclear whether CyP inhibitors have therapeutic potential in DMD patients. Here we report (i) the presence of a PTP-dependent mitochondrial defect and (ii) the therapeutic effect of alisporivir in both muscle-derived primary cell cultures from DMD patients and in the *sapje* zebrafish, a severe model of DMD [30].

2. Materials and methods

2.1. Muscle cell cultures

Muscle biopsies were obtained from healthy donors and DMD patients. DMD patient 1 had a deletion of exons 48–54 (out of frame deletion), DMD patient 2 a c5551 C > T stop mutation in exon 39, and DMD patient 3 a deletion of exons 48–50 (out of frame deletion). Cultures were prepared by enzymatic and mechanical treatment of muscle biopsies and by plating in Dulbecco's modified Eagle's medium (DMEM) supplemented with 20% fetal calf serum, penicillin, streptomycin and amphotericin B (Sigma) as previously described [31] and stored in liquid nitrogen. Cells were expanded and used within the 7th passage.

2.2. Measurement of mitochondrial membrane potential

Mitochondrial membrane potential was measured based on the accumulation of tetramethylrhodamine methyl ester (TMRM). Cells were seeded onto 24 mm diameter round glass coverslips and grown for two days in DMEM supplemented with 20% fetal calf serum. To normalize the loading conditions, in all experiments with TMRM the medium was supplemented with 1.6 μM CsH, which inhibits the multi-drug resistance pump but not the PTP [32]. Cells were rinsed once and then incubated in serum-free DMEM supplemented with 1.6 μM CsH and loaded with 10 nM TMRM for 30 min. At the end of each experiment, mito-

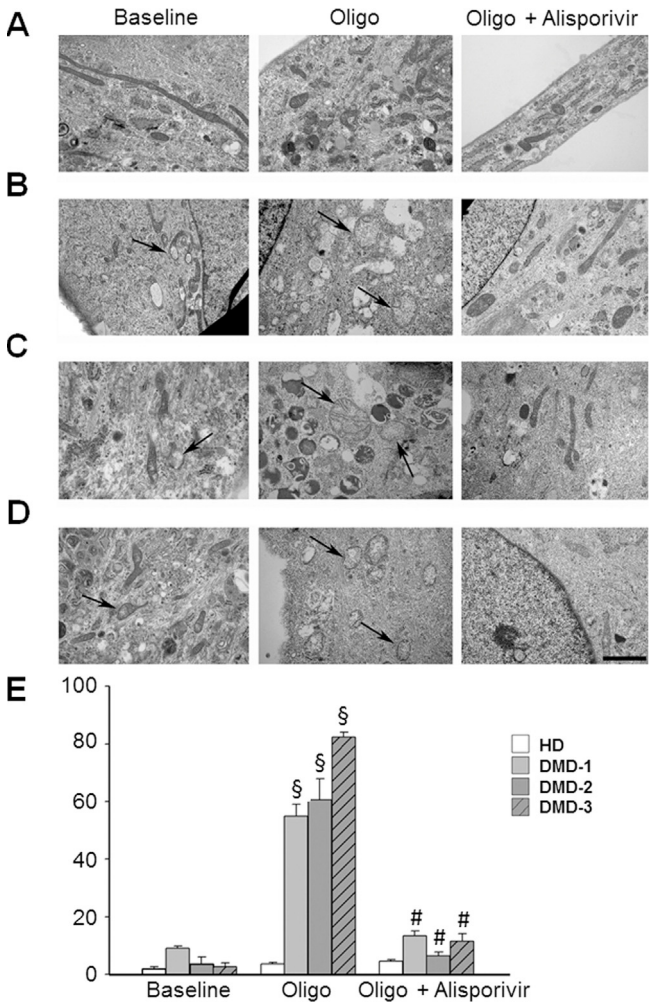

Fig. 2. Effects of oligomycin and alisporivir on mitochondrial ultrastructure in healthy donor and DMD patient primary muscle cell cultures. Electron micrographs of muscle cell cultures from (**A**) a healthy donor, (**B**) DMD patient 1, (**C**) DMD patient 2 and (**D**) DMD patient 3 plated in the absence (left panels) or after treatment for 90 min with 6 μM oligomycin (central panels) or 6 μM oligomycin plus 1.6 μM alisporivir (right panels). A few swollen mitochondria (arrows) could occasionally be found in the cells of DMD patients. Treatment with oligomycin caused mitochondrial swelling in the majority of cells from all patients but not healthy donor cells, and the effect of oligomycin could be prevented by treatment with alisporivir. Scale bar, 1 μm. (**E**), statistical analysis of occurrence of swollen mitochondria; values on the ordinate refer to the percentage of cells with swollen mitochondria and analysis was performed on 300 cells per condition. § $p < 0.001$, samples treated with oligomycin compared to the baseline; # $p < 0.001$, samples treated with oligomycin compared to the samples treated with oligomycin + alisporivir; 2-way ANOVA with Bonferroni correction.

chondria were fully depolarized by the addition of 4 μM of the protonophore carbonylcyanide-*p*-trifluoromethoxyphenyl hydrazone (FCCP). Cellular fluorescence images were acquired with an Olympus IX71/IX51 inverted microscope, equipped with a xenon light source (150 W) for epifluorescence illumination, and with a digital camera. For detection of fluorescence, 545 ± 15 nm bandpass excitation and 572 nm longpass emission filter settings were used. Images were collected with exposure time of 100 msec using a 40x, 1.3 NA oil immersion objective (Olympus). Data were acquired and analyzed using Cell R software (Olympus). Clusters of several mitochondria (10–30) were identified as regions of interest, and fields not containing cells were taken as the background. Sequential digital images were acquired every 2 or 5 min as specified in the figure legends. Average fluorescence intensity of all relevant regions was recorded and stored for subsequent analysis.

2.3. Measurement of oxygen consumption rate

Oxygen consumption rates (OCR) were measured with the Seahorse XF-24 extracellular flux analyzer, which detects oxygen consumption through a sensor cartridge embedded with a fluorescent sensor for oxygen. The sensor is coupled to a fiber-optic waveguide, which delivers light at 532 nm and transmits a fluorescent signal to highly sensitive photodetectors through optical filters [33]. Muscle-derived cell cultures were seeded in XF-24 cell culture plates at 2.5×10^4 cells/well in 0.2 ml of DMEM with 20% fetal calf serum, penicillin, streptomycin and incubated at 37 °C in 5% CO_2 for 24 h. Assays were initiated by replacing the growth medium with serum-free DMEM and the experiment was performed at 37 °C. The optimal concentration of FCCP required for maximal stimulation of respiration, which ranged between 0.4 and 1 μM, was routinely determined by titration. After a stable OCR baseline was established, oligomycin, FCCP, rotenone and antimycin A were added as specified in the figure legends. Zebrafish embryos at 72 h post fertilization (hpf) were staged and placed into the wells of an XF-24 capture microplate (1 embryo per well). Capture screens were placed on top of the embryos in order to keep them in place under the measurement area and each well was filled with 670 μl of fish water (0.5 mM NaH_2PO_4, 0.5 mM $NaHPO_4$, 3 mg/l instant ocean). The surface area of the sensor is much smaller than that of the embryos, and detection of respiration occurs in the region immediately below the sensor itself making the measurements independent of embryo size. The experiment was performed at 28.5 °C and an OCR baseline was established for 40 min. Respiratory rates are average ± SEM of at least 20 individual embryos per condition.

2.4. Zebrafish and embryo maintenance

Adult zebrafish were maintained in the Department of Biology Facility of the University of Padova in aerated saline water according to standard protocols under a 14 h light – 10 h dark cycle at 28.5 °C. Males and females were separated in the late afternoon and the next morning were freed to start courtship, which ended with egg deposition and fecundation. Eggs were collected, washed with fish water (0.5 mM NaH_2PO_4, 0.5 mM $NaHPO_4$, 0.2 mg/l methylene blue, 3 mg/l instant ocean) and maintained at 28.5 °C in fish water supplemented with an antibiotic-antimycotic cocktail (50 μg/ml ampicillin, 100 units/ml penicillin and 0.1 mg/ml streptomycin, Biochrom, 3.3 μg/ml amphotericin B, Bristol-Myers-Squibb). $dmd^{ta222a/+}$ stable mutants carrying a point mutation (A > T) in exon 4 of the *dmd* gene (located in zebrafish chromosome 1) were kindly provided by the Karlshrue Institute of Technology (KIT, Karlshrue, Germany). Since the homozygous mutants died by 9 dpf, heterozygotes were used to keep and expand the line. Homozygotes were obtained at the expected Mendelian ratio by crossing heterozygotes, identified through a birefringence screening at 48 hpf and used for experiments.

2.5. Zebrafish drug treatment

Mutant embryos were dechorionated at 20 hpf and then treated with drugs starting at 48 hpf. Alisporivir and CsA (Debiopharm, Lausanne, Switzerland) were used at the indicated concentrations and dissolved in 0.01% DMSO in fish water. Vehicle control treatment consisted of 0.01% DMSO in fish water. Larvae birefringence was analyzed at 5 days post fertilization (dpf) and fish survival observed between 3 and 30 dpf. Effects of long-term alisporivir treatment were evaluated by counting the number of surviving larvae.

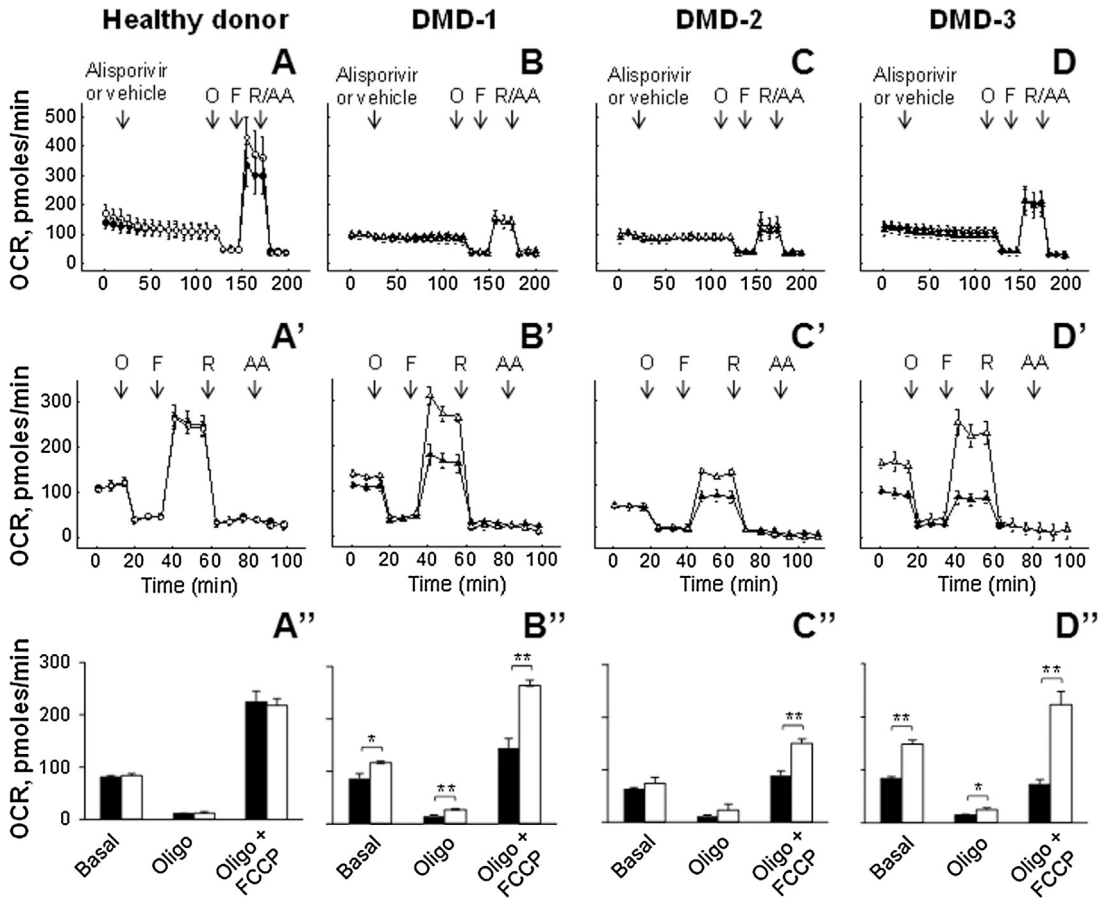

Fig. 3. Oxygen consumption rate of primary muscle cell cultures derived from healthy donor and DMD patients. Oxygen consumption rate (OCR) of primary muscle cell cultures from a healthy donor (closed circles in panel **A** and **A'**) and from DMD patients (closed triangles) 1 (panel **B-B'**), 2 (panel **C-C'**), and 3 (panel **D-D'**) was measured in 24-well Seahorse plates [35,000 cells per well^{-1}]. Where indicated (arrows) 1 μM alisporivir (open symbols) or vehicle (closed symbols), 1 μg × ml^{-1} oligomycin (O), 0.4–1.0 μM FCCP to achieve maximal respiration as assessed in independent titrations (F), 1 μM rotenone (R), and 1 μM antimycin A (AA) were added. In panels A'-D' open symbols report respiration of primary muscle cell cultures treated with 1 μM alisporivir for 2 weeks before the recording. Statistics of mitochondrial OCR of primary muscle cell cultures from healthy donor (**A"**) and patients (**B"-D"**) treated for 2 weeks with vehicle (closed bars) or 1 μM alisporivir (open bars) before (Basal) and after the sequential addition of oligomycin Oligo) and FCCP (Oligo + FCCP). Data are mean of at least three independent experiments ± SEM and nonmitochondrial respiration (OCR after addition of antimycin A) was subtracted. (*$p < 0.05$; **$p < 0.005$) 2-tailed Student's *t* test.

2.6. Birefringence assay

Muscle birefringence was analyzed at 48 hpf to screen the embryos with *dmd*$^{ta222a/ta222a}$ genotype, and at 5 dpf to evaluate the effect of alisporivir on muscle integrity. Briefly, embryos were anesthetized with 0.02% tricaine (SIGMA Aldrich, St. Louis, MO, USA) in Tris-Cl pH 9.1, embedded in 2% methylcellulose (SIGMA Aldrich, St. Louis, MO, USA), placed on glass and finally analyzed for muscle light refraction with polarizing filters with a Leica M165FC stereomicroscope. We calculated the integrated area of birefringence pixels by using ImageJ software, as described [34]. In the scoring reported in Fig. 7A, birefringence values of 2×10^6 (typical of wild-type individuals) were considered normal, values between 1.9 and 0.6×10^6 indicative of a mild alteration and values of 0.6×10^6 of a severe alteration.

2.7. Genotyping

DNA was extracted from whole embryos or tails at 5 and 30 dpf, respectively. Lysis was performed using 10 μg/ml proteinase K in Tris-HCl buffer pH 8.0 and DNA was precipitated with NaOAc 3 M pH 5.2 in EtOH 100%. To genotype embryos and larvae, a PCR with primers specific for the *dmd* gene was performed. PCR samples were sequenced by bmr-genomics sequencing service (Padova, Italy).

2.8. Ultrastructural analysis

Wild-type and *sapje* zebrafish embryos were fixed with Karnovsky fixative (2.5% glutaraldehyde and 2% paraformaldheyde in 0.1 M cacodylate buffer) for 3 h at 4 °C, washed with 0.1 M cacodylate buffer, post-fixed with osmium tetroxide for 2 h, and embedded in EPON 812 as previously described [26]. Muscle cell cultures were washed with PBS, fixed with 2.5% glutaraldehyde in 0.1 M phosphate buffer (pH 7.4) and postfixed with 1% osmium tetroxide in veronal buffer. Samples were detached from the plastic dish with propylene oxide, centrifuged, and embedded in Epon E812 resin. Ultrathin sections were stained with uranyl acetate and lead citrate and observed with a Philips (Eindhoven, the Netherlands) EM400 electron microscope at 100 kV. For the determination of the percentage of cells with swollen mitochondria, three hundred cells were examined for each sample, while necrotic aspects were excluded.

2.9. Statistical analysis

Data were analyzed using 1-way ANOVA with Bonferroni correction and 2-tailed Student's *t*-test. Values with $p < 0.05$ were considered significant and data are reported as mean ± SEM.

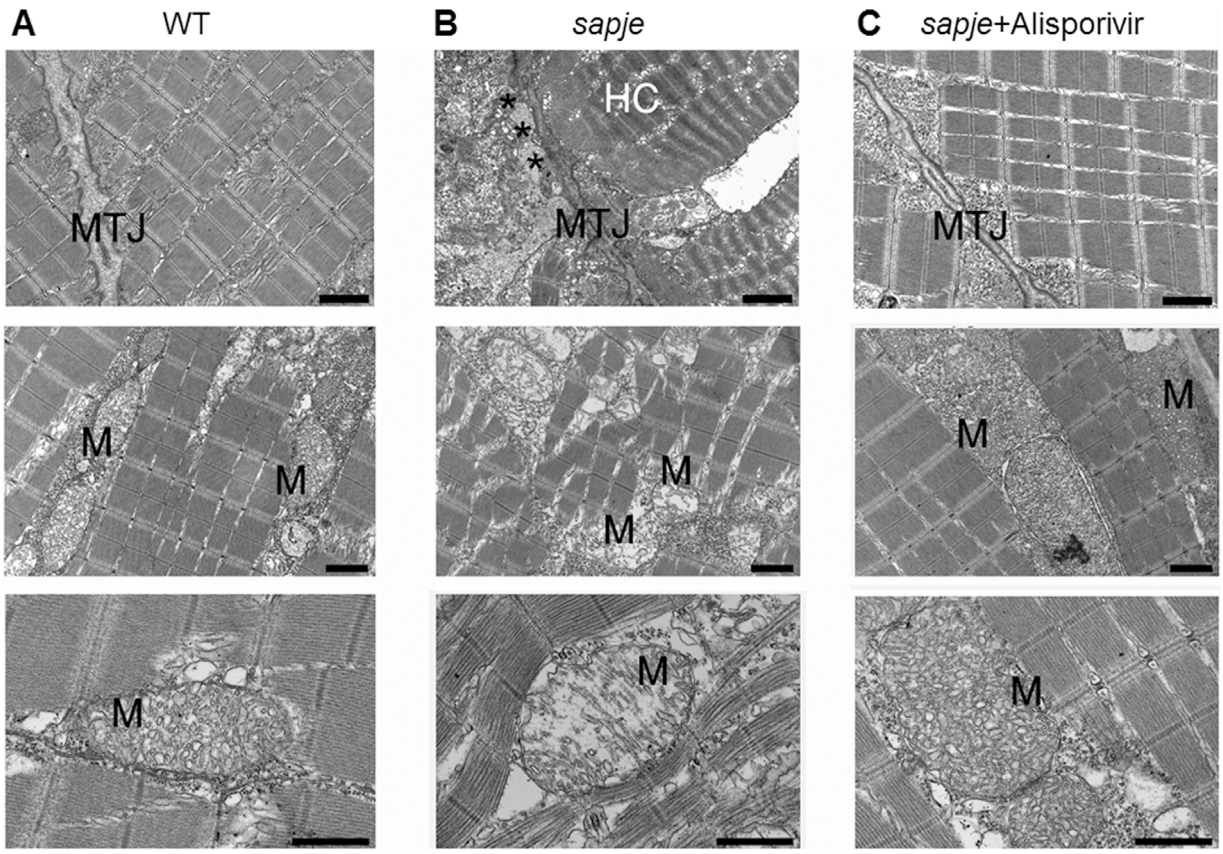

Fig. 4. Ultrastructure of wild-type and *sapje* zebrafish at 3 dpf. Effect of alisporivir on the *sapje* genotype. (**A**) Wild-type (WT, left panels), (**B**) *sapje* zebrafish (middle panels) and (**C**) *sapje* zebrafish treated with 5 μM alisporivir starting at 48 hpf (right panels) were studied at 3 dpf. Wild-type embryos form a regular sarcomeric array that attaches obliquely to the myotendinous junction (MTJ) (**A**, upper panel); inter and sub-sarcolemmal mitochondria with well developed cristae are detected (**A**, middle and lower panel). In *sapje* embryos, several fibers show myofibril detachment (asterisks) from the MTJ, and display hyper-contracted areas (HC) (**B**, upper panel). Compared to wild-type (**A**, middle and lower panels), in the *sapje* zebrafish mitochondria (M) appear enlarged, with reduced number of cristae and matrix density (**B**, middle and lower panel). The treatment with alisporivir rescued the attachment of myofibrils to the MTJ (**C**, upper panel) and the mitochondrial cristae organization (**C**, middle and lower panels). Scale bar, 1 μm.

2.10. Study approval

Healthy donors and DMD patients provided informed consent and the study was approved by the ethical committee of the Rizzoli Orthopaedic Institute, Bologna. Studies on zebrafish were approved by the Italian Health Ministry – Animal Health and Veterinarian Drugs (protocol n. 414/2015 PR of 21-5-2015).

3. Results

We assessed the response of muscle cell cultures from DMD patients to the F_1F_O-ATP synthase inhibitor oligomycin, a method that we have used to unmask the latent mitochondrial dysfunction of patients and mice with collagen VI myopathies [22–25,35]. After the initial increase of TMRM uptake due to hyperpolarization, oligomycin caused mitochondrial depolarization (which is usually due to Ca^{2+} deregulation linked to ATP depletion [36]) only in the cells from DMD patients (Fig. 1B–D, compare with A; similar results were obtained from an additional healthy donor, data not shown; see ref [37] for the response of 2 additional DMD patients). Although some variability in the response of individual cells is apparent, in the majority of the patient cells alisporivir prevented or slowed down depolarization, suggesting that the latter was due to PTP opening (Fig. 1B'–D').

Mitochondria from patient cultures occasionally displayed abnormal morphology (Fig. 2B-D, left panels). Treatment with oligomycin caused mitochondrial swelling in all patient cultures (Fig. 2B–D, middle panels) and this predicted effect of PTP opening was prevented by alisporivir (Fig. 2B–D, right panels). Oligomycin-induced mitochondrial abnormalities were not detected in cells from healthy donor (Fig. 2A), while they were present in the majority of cells from DMD patients (Fig. 2E). These findings indicate that cells from DMD patients have a latent mitochondrial dysfunction that can be unmasked by treatment with oligomycin.

Cellular respiration is largely due to ATP synthesis, and the fraction of oxygen consumption linked to phosphorylation can be assessed by inhibiting the F_1F_O-ATP synthase with oligomycin. Basal respiration was the same in cultures from the healthy donor and the DMD patients, as was the response to oligomycin (Fig. 3A–D; results similar to those depicted in panel A were obtained from an additional healthy donor, omitted for clarity). These findings suggest that in resting cells oxidative phosphorylation provides enough ATP irrespective of the genotype. A striking difference emerged upon addition of the protonophore FCCP. At variance from healthy donor, cells from DMD patients displayed a very small respiratory increase, i.e. they had a small respiratory reserve (Fig. 3A–D). Acute treatment with alisporivir did not improve maximal respiration (compare closed and open symbols in Fig. 3A–D). We reasoned that some consequences of increased PTP opening may not be readily reversible. We therefore treated cells with alisporivir for 2 weeks before assessing oxygen consumption and its response to oligomycin and FCCP. Cells from all DMD patients now displayed increased maximal respiratory capacity, a

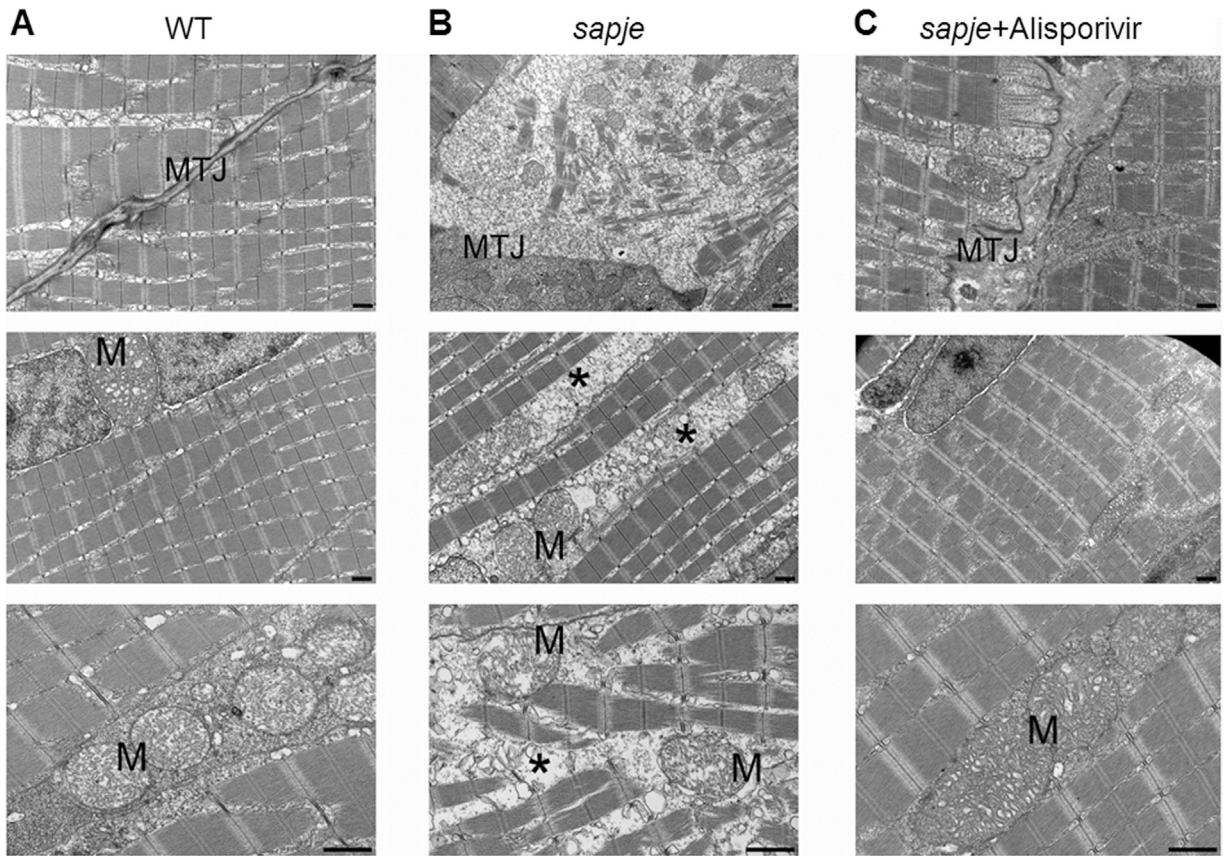

Fig. 5. Ultrastructure of wild-type and *sapje* zebrafish at 8 dpf. Effect of alisporivir on the *sapje* genotype. (**A**) Wild-type (WT, left panels), (**B**) *sapje* (middle panels) and (**C**) *sapje* treated with 5 μM alisporivir (right panels) zebrafish were studied at 8 dpf. Well formed myotendinous junction (MTJ), regular sarcomeric array and mitochondria (M) with well developed cristae characterize the wild-type fibers (**A**). *sapje* zebrafish display prominent loss of myofilaments near the MTJ with frequent detachments (asterisks) and marked mitochondrial alterations (detachment of the outer membrane and disrupted cristae) (**B**). Treatment with alisporivir improved the overall morphology of myofibrils and mitochondria (**C**). Scale bar, 1 μm.

result that was particularly clear-cut for cells from patients 1 and 3 (Fig. 3A'–D' and A"–D").

To assess the effects of alisporivir *in vivo* we chose the *sapje* zebrafish [38], which carries an A > T transversion within exon 4 of *dmd* in autosomal chromosome 1. This causes a nonsense mutation at position K76 that segregates in the homozygous state with the *sapje* phenotype [39]. Wild-type embryos at 3 dpf displayed a regular sarcomeric array that attaches obliquely to the myotendinous junction (MTJ) and both interfibrillar and subsarcolemmal mitochondria with well developed cristae (Fig. 4A). In *sapje* embryos several fibers showed detachment of the myofibrils from the MTJ and hyper-contracted areas. Mitochondria appeared enlarged, with reduced number of cristae and decreased matrix density (Fig. 4B). Treatment with alisporivir rescued the attachment of myofibrils to the MTJ and mitochondrial cristae organization (Fig. 4C). At 8 dpf the wild-type zebrafish had well formed MTJ, with a regular array of sarcomeres and mitochondria (Fig. 5A), while *sapje* zebrafish displayed prominent loss of myofilaments near the MTJ, frequent fiber detachments and marked mitochondrial alterations with outer membrane dilations and disrupted cristae (Fig. 5B). Treatment with alisporivir improved fiber attachment to the MTJ and overall myofibril morphology, and normalized mitochondrial ultrastructure (Fig. 5C). The mitochondrial defects were detected also in non-degenerating myofibers (Fig. 5B, middle panel), suggesting an early involvement of mitochondria in the progression of *sapje* muscle pathology. Interestingly, mitochondrial alterations were detected in fast glycolytic but not slow oxidative fibers (Fig. 6, compare A and B). This finding is extremely relevant because it matches the relative resistance of slow oxidative fibers to disease reported in DMD patients [40]. Treatment with alisporivir but not with CsA ameliorated *in vivo* muscle birefringence, a direct measurement of muscle organization. At a concentration of 5 μM alisporivir was able to rescue the normal phenotype in 60% of the *sapje* zebrafish up from a basal level of about 5% (Fig. 7A). The beneficial effects of alisporivir were also apparent from analysis of overall birefringence, which was improved at 5 and 10 μM (Fig. 7B). It should be noted that the effect alisporivir displayed a bell-shaped curve with decreased efficacy at 10 μM.

We next performed respiratory measurements in living zebrafish and found that the basal respiratory rate (which is coupled to oxidative phosphorylation) was lower in *sapje* than in wild-type zebrafish (Fig. 7C). Treatment with 5 μM alisporivir partially restored basal OCR while *sapje* embryos treated with 5 μM CsA showed an OCR comparable to that of untreated embryos (Fig. 7C). In keeping with a causative role of mitochondrial dysfunction in muscle demise and early death of the dystrophic *sapje* zebrafish, treatment with alisporivir shifted 50% survival from 11 to 16.5 days, with 20% of alisporivir-treated fish still surviving at 30 days (Fig. 7C). On the other hand, treatment with CsA worsened *sapje* zebrafish survival (Fig. 7D). This finding indicates that inhibition of calcineurin has detrimental consequences in zebrafish disease progression, a finding that matches the results obtained in other animal models [40–42] and in DMD patients [43,44].

4. Discussion

The general idea that fiber death in muscle diseases is caused by increased sarcolemmal Ca^{2+} flux triggering a vicious cycle of

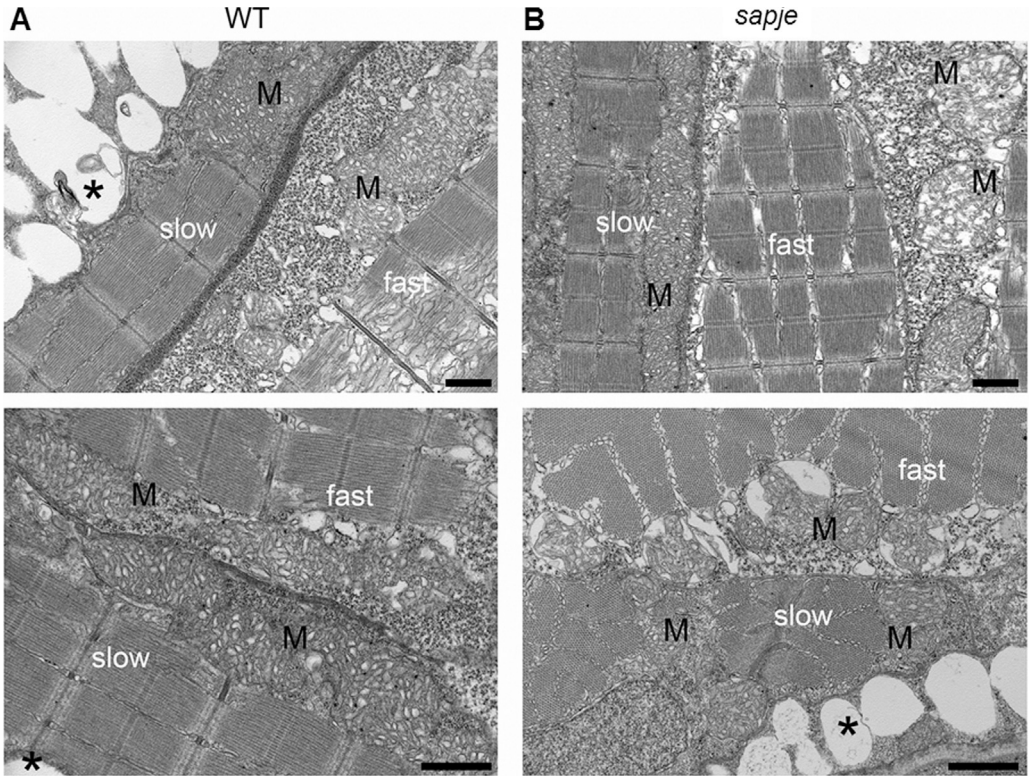

Fig. 6. Ultrastructure of mitochondria in slow (oxidative) and fast (glycolytic) fibers of wild-type and *sapje* zebrafish. Slow oxidative fibers (slow) are located under skin cells (asterisks), while fast glycolytic fibers (fast) are underneath the slow muscles (images taken at 3 dpf). (**A**) In wild-type (WT) embryos mitochondria (M) of slow and fast fibers display minimal morphological differences. (**B**) In *sapje* zebrafish only mitochondria of fast fibers are swollen while mitochondria of slow fibers are preserved and display well organized cristae. Scale bar, 1 μm.

mitochondrial Ca^{2+} overload and ATP depletion was first proposed forty years ago [18]. The excess Ca^{2+} uptake would initially be compensated, but over time it would cause structural damage to mitochondria followed by decreased ATP production, worsening of the cytosolic [Ca^{2+}] increase and eventually hypercontracture and fiber death. Consistent with this idea, mitochondria from myopathic animals were not different from those of healthy individuals [45,46], but contained more Ca^{2+} [47,48] and were sensitive to a Ca^{2+}-dependent decrease in respiration and ATP production with NAD^+-linked substrates [49]. It is now well documented (i) that increased cytosolic/organellar [Ca^{2+}] causes muscle pathology *per se* in otherwise healthy individuals [7], as demonstrated by genetic manipulation of TRPC3 channels [50], SERCA1 and 2a [51], ORA1/STIM1 [52], NCX1 [53] or by treatment with cardiotoxin [54]; and (ii) that a key effector mechanism is opening of the Ca^{2+}-dependent mitochondrial PTP [8]. Due to their proximity to the sarcoplasmic reticulum, mitochondria take up Ca^{2+} even under resting conditions [55–58] in a process that is sensitive to redox events [59,60]. Thus, mitochondria can be affected by deregulation of Ca^{2+} homeostasis [48] even when cytosolic [Ca^{2+}] appears to be normal [15,61], i.e. in the early stages of muscular dystrophies when the defect is compensated [7]. Increase of the PTP open time may then gradually decrease ATP production and cause secondary dysfunction of the sarcoplasmic reticulum resulting in further increase of mitochondrial matrix Ca^{2+} and setting up a self-amplifying vicious circle eventually causing fiber demise [8,18]. Pathogenic factors are also Ca^{2+}-dependent calpain activation [13] and excess reactive oxygen and nitrogen species, which have synergistic effects with those of Ca^{2+} overload [62–64].

Prolonged PTP opening causes depolarization, thus preventing ATP synthesis and promoting hydrolysis of any available glycolytic ATP. Owing to the PTP exclusion size of about 1.5 kDa, matrix solutes equilibrate and matrix NAD^+ is lost causing inhibition of respiration [65,66], one of the defining features of the latent mitochondrial dysfunction of dystrophic muscle [49]. Upon release from the matrix, NAD^+ undergoes rapid cleavage by outer membrane glycohydrolase [67] and in mammals it cannot be imported from the cytosol [68]. Restoration of the mitochondrial NAD^+ pool thus requires *de novo* synthesis [69] and it appears plausible that the time required to recover respiration after treatment with alisporivir reflects the time required for NAD^+ synthesis from nicotinamide mononucleotide [70]. At least in the *mdx* mouse, ATP production may also be compromised by decreased oxidative utilization of glucose and free fatty acids [71], and decreased levels of respiration [72–74] may even precede the Ca^{2+}-dependent damage due to dystrophin deficiency in the myofibers [73]. Partial restoration of respiration with alisporivir in DMD patient cells and *sapje* zebrafish is important because it suggests that decreased rates of respiration (hence ATP production) may contribute to muscle weakness in the patients. Recovery of muscle strength could therefore be an early indication of efficacy during alisporivir treatment.

The features of the PTP in zebrafish are superimposable to those of mammals [75] and the *sapje* zebrafish is an excellent model of DMD [38]. In *sapje* homozygotes, fibers show detached ends and shortening, with reduced separation and regularity of sarcomeric banding, and nuclear condensation indicative of apoptosis [39]. As shown here, mitochondria are selectively affected in fast glycolytic fibers, while mitochondria from slow oxidative fibers appear preserved, a finding that matches the propensity of fiber subtypes to undergo demise in DMD patients [40]. An unexpected effect of alisporivir in the *sapje* zebrafish was the recovered alignment of myofibrils at the MTJ, which apparently drove the reconstitution of muscle structure and the substantial amelioration of motility and survival. It should be recalled that early alterations of the

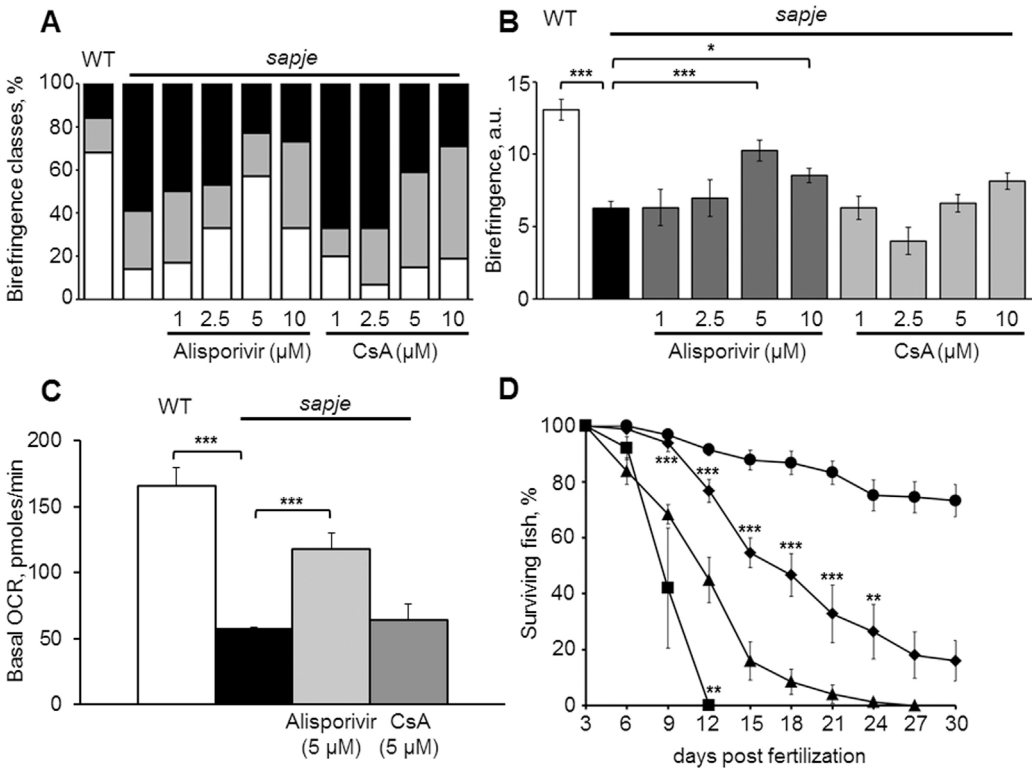

Fig. 7. Effect of alisporivir on birefringence, respiration and survival of *sapje* zebrafish. Zebrafish were treated at 48 hpf with 0.6% DMSO or, where indicated, with alisporivir or CsA dissolved in 0.6% DMSO; WT, wild-type. (**A, B**) Birefringence analysis of zebrafish phenotpyes (normal, open bars; moderate, grey bars; severe, black bars, see Materials and Methods for scoring details) (**A**) and statistical analysis of birefringence measured as pixel-integrated density areas (**B**) at 5 dpf. Data in (**B**) represent the mean of at least three independent experiments ± SEM, $^{*}p < 0.05$, $^{***}p < 0.001$. Total embryos were: wild-type, 48; untreated *sapje*, 42; *sapje* treated with 1, 2.5, 5 and 10 μM alisporivir, 18, 21, 43 and 42, respectively; *sapje* treated with 1, 2.5, 5 and 10 μM CsA, 16, 18, 22 and 20, respectively. (**C**) Oxygen consumption rate (OCR) was recorded for 40 min at 3 dpf. Total embryos were: wild-type, 33; *sapje* untreated, 27; *sapje* treated with 5 μM alisporivir or CsA for 24 h, 21 and 11, respectively. Data are mean of six independent experiments ± SEM. ($^{***}p < 0.001$, 1-way ANOVA with Bonferroni correction). (**D**) Zebrafish were observed every 3 days and the number of surviving fish counted from 3 to 30 dpf. Percentage of surviving fish is reported for untreated wild-type (closed circles), *sapje* (closed triangles) and *sapje* treated with 5 μM CsA (closed squares) or 5 μM alisporivir (closed diamonds). Data represent the mean of three independent experiments. Error bars refer to the SEM. For each experiment total number of embryos used was 60. Asterisks denote statistically significant differences between untreated and treated *sapje* zebrafish $^{**}p < 0.01$, $^{***}p < 0.001$, 1-way ANOVA with Bonferroni correction.

MTJ (including the presence of abnormal mitochondria) had been detected in dystrophic Davis chicken as early as at 13 d *in ovo* [76] and in *mdx* mice, where the alterations preceded necrosis and played a significant role in development of the dystrophic phenotype [77–79]. Restoration by alisporivir of normal muscle MTJ and morphogenesis in *sapje* zebrafish reveals a hitherto unsuspected feedback between mitochondrial function and correct development of muscle during embryogenesis.

Gene ablation studies have shown that calcineurin plays an important role during myogenesis and fiber type switching [80,81], a good explanation for why NIM811 (which like alisporivir does not affect calcineurin) is superior to CsA in the treatment of the severe collagen VI muscular dystrophy in zebrafish [25,26]. It is remarkable that α-actinin-3 deficiency stimulates oxidative muscle metabolism through activation of calcineurin [43,44], which decreases overall muscle performance but slows down disease progression by favoring fiber switch towards the more disease-resistant slow oxidative type [44]; and that tamoxifen, which significantly counteracts pathology in the *mdx* mouse model, enhances calcineurin expression in the *gastrocnemius* muscle, suggestive of a fast-to-slow phenotypic transition [82]. Our results suggest that the potential protective effect of CsA through CyPD inhibition is offset by the detrimental consequences of calcineurin inhibition. These findings may explain why CsA gave contradictory results in clinical trials in DMD patients [83–85], which may also depend on the different drug doses used.

The effective concentrations of alisporivir are higher than those needed to fully inhibit the enzymatic activity of CyPs by CsA *in vitro*, which is in the low nanomolar range [86]. This discrepancy can be partly explained by equilibration across several membranes and by binding to other isoforms like the abundant cytosolic CyPA and the endoplasmic reticulum CyPB. The latter interaction may also contribute to explain the bell-shaped effect of alisporivir because CyPB affects Ca^{2+} homeostasis through the calcium-modulating cyclophilin ligand CAML [87]. First identified in T lymphocytes, this protein is ubiquitously expressed and has a prosurvival function in lymphocytes [87] and possibly in muscle cells, an issue that deserves further study. Yet, the significant correction of the mitochondrial and structural defects, the substantial recovery of respiration in both patient cells and zebrafish and the increased survival of dystrophic *sapje* zebrafish by alisporivir treatment raise hopes for the therapy of DMD. Besides *mdx* mice [27], solid evidence that the PTP is involved in disease pathogenesis exists for *Scgd*$^{-/-}$ mice [27] (which lack δ sarcoglycan and are a model of limb-girdle muscular dystrophy) [88], *Lama2* mice [27] (which lack laminin 2 and are a model of congenital muscular dystrophy) [88] and *Col6a1*$^{-/-}$ mice [22] (which lack collagen VI and are a model of Ullrich and Bethlem muscular dystrophies) [89]. Alisporivir was generally well tolerated in HCV patients [90,91] and the current results indicate that it could be used in the treatment of DMD and possibly of other muscular dystrophies.

Conflict of interest

None.

Acknowledgments

This work was supported by Italian Telethon Foundation (GGP14037). We would like to thank Francesca Sardone for help with the preparation of human cell cultures. We gratefully acknowledge the Zebrafish Facility at the Department of Biology, University of Padova and Debiopharm SA, Lausanne for the generous gift of alisporivir.

References

[1] M. Koenig, E.P. Hoffman, C.J. Bertelson, A.P. Monaco, C. Feener, et al., Complete cloning of the Duchenne muscular dystrophy (DMD) cDNA and preliminary genomic organization of the DMD gene in normal and affected individuals, Cell 50 (1987) 509–517.
[2] R.H. Hoffman, L.M. Brown Jr., Dystrophin: the protein product of the Duchenne muscular dystrophy locus, Cell 51 (1987) 919–928.
[3] K.P. Campbell, S.D. Kahl, Association of dystrophin and an integral membrane glycoprotein, Nature 338 (1989) 259–262.
[4] S. Guiraud, A. Aartsma-Rus, N.M. Vieira, K.E. Davies, G.J. van Ommen, et al., The pathogenesis and therapy of muscular dystrophies, Annu. Rev. Genomics Hum. Genet. 16 (2015) 281–308.
[5] J.M. Ervasti, K.P. Campbell, A role for the dystrophin-glycoprotein complex as a transmembrane linker between laminin and actin, J. Cell Biol. 122 (1993) 809–823.
[6] I.N. Rybakova, J.R. Patel, J.M. Ervasti, The dystrophin complex forms a mechanically strong link between the sarcolemma and costameric actin, J. Cell Biol. 150 (2000) 1209–1214.
[7] A.R. Burr, J.D. Molkentin, Genetic evidence in the mouse solidifies the calcium hypothesis of myofiber death in muscular dystrophy, Cell Death Differ. 22 (2015) 1402–1412.
[8] A. Zulian, M. Schiavone, V. Giorgio, P. Bernardi, Forty years later: mitochondria as therapeutic targets in muscle diseases, Pharmacol. Res. 113 (2016) 563–573.
[9] J.B. Bodensteiner, A.G. Engel, Intracellular calcium accumulation in Duchenne dystrophy and other myopathies: a study of 567,000 muscle fibers in 114 biopsies, Neurology 28 (1978) 439–446.
[10] C.A. Maunder-Sewry, R. Gorodetsky, R. Yarom, V. Dubowitz, Element analysis of skeletal muscle in Duchenne muscular dystrophy using x-ray fluorescence spectrometry, Muscle Nerve 3 (1980) 502–508.
[11] M.J. Jackson, D.A. Jones, R.H. Edwards, Measurements of calcium and other elements in muscle biopsy samples from patients with Duchenne muscular dystrophy, Clin. Chim. Acta 147 (1985) 215–221.
[12] P.R. Turner, T. Westwood, C.M. Regen, R.A. Steinhardt, Increased protein degradation results from elevated free calcium levels found in muscle from *mdx* mice, Nature 335 (1988) 735–738.
[13] M.J. Spencer, D.E. Croall, J.G. Tidball, Calpains are activated in necrotic fibers from mdx dystrophic mice, J. Biol. Chem. 270 (1995) 10909–10914.
[14] N. Imbert, C. Cognard, G. Duport, C. Guillou, G. Raymond, Abnormal calcium homeostasis in Duchenne muscular dystrophy myotubes contracting in vitro, Cell Calcium 18 (1995) 177–186.
[15] J.M. Gillis, Membrane abnormalities and Ca homeostasis in muscles of the mdx mouse, an animal model of the Duchenne muscular dystrophy: a review, Acta Physiol. Scand. 156 (1996) 397–406.
[16] N. Mallouk, V. Jacquemond, B. Allard, Elevated subsarcolemmal Ca^{2+} in *mdx* mouse skeletal muscle fibers detected with Ca^{2+}-activated K+ channels, Proc. Natl. Acad. Sci. U. S. A 97 (2000) 4950–4955.
[17] N. Mallouk, B. Allard, Ca^{2+} influx and opening of Ca^{2+}-Activated K^+ channels in muscle fibers from control and *mdx* mice, Biophys. J. 82 (2002) 3012–3021.
[18] K. Wrogemann, S.D. Pena, Mitochondrial calcium overload: a general mechanism for cell-necrosis in muscle diseases, Lancet 1 (1976) 672–674.
[19] V. Giorgio, V. Burchell, M. Schiavone, C. Bassot, G. Minervini, et al., Ca^{2+} binding to F-ATP synthase beta subunit triggers the mitochondrial permeability transition, EMBO Rep. 18 (2017) 1065–1076.
[20] P.C. Waldmeier, J.J. Feldtrauer, T. Qian, J.J. Lemasters, Inhibition of the mitochondrial permeability transition by the nonimmunosuppressive cyclosporin derivative NIM811, Mol. Pharmacol. 62 (2002) 22–29.
[21] M.J. Hansson, G. Mattiasson, R. Mansson, J. Karlsson, M.F. Keep, et al., The nonimmunosuppressive cyclosporin analogs NIM811 and UNIL025 display nanomolar potencies on permeability transition in brain-derived mitochondria, J. Bioenerg. Biomembr. 36 (2004) 407–413.
[22] W.A. Irwin, N. Bergamin, P. Sabatelli, C. Reggiani, A. Megighian, et al., Mitochondrial dysfunction and apoptosis in myopathic mice with collagen VI deficiency, Nat. Genet. 35 (2003) 267–271.
[23] T. Tiepolo, A. Angelin, E. Palma, P. Sabatelli, L. Merlini, et al., The cyclophilin inhibitor Debio 025 normalizes mitochondrial function, muscle apoptosis and ultrastructural defects in *Col6a1*$^{-/-}$ myopathic mice, Br. J. Pharmacol. 157 (2009) 1045–1052.
[24] A. Angelin, T. Tiepolo, P. Sabatelli, P. Grumati, N. Bergamin, et al., Mitochondrial dysfunction in the pathogenesis of Ullrich congenital muscular dystrophy and prospective therapy with cyclosporins, Proc. Natl. Acad. Sci. U. S. A. 104 (2007) 991–996.
[25] A. Zulian, E. Rizzo, M. Schiavone, E. Palma, F. Tagliavini, et al., NIM811, a cyclophilin inhibitor without immunosuppressive activity, is beneficial in collagen VI congenital muscular dystrophy models, Hum. Mol. Genet. 23 (2014) 5353–5363.
[26] W.R. Telfer, A.S. Busta, C.G. Bonnemann, E.L. Feldman, J.J. Dowling, Zebrafish models of collagen VI-related myopathies, Hum. Mol. Genet. 19 (2010) 2433–2444.
[27] D.P. Millay, M.A. Sargent, H. Osinska, C.P. Baines, E.R. Barton, et al., Genetic and pharmacologic inhibition of mitochondrial-dependent necrosis attenuates muscular dystrophy, Nat. Med. 14 (2008) 442–447.
[28] O.M. Reutenauer, O. Dorchies, G. Patthey-Vuadens, U.T. Vuagniaux, Investigation of Debio 025, a cyclophilin inhibitor, in the dystrophic *mdx* mouse, a model for Duchenne muscular dystrophy, Br. J. Pharmacol. 155 (2008) 574–584.
[29] E.R. Wissing, D.P. Millay, G. Vuagniaux, J.D. Molkentin, Debio-025 is more effective than prednisone in reducing muscular pathology in *mdx* mice, Neuromuscul. Disord. 20 (2010) 753–760.
[30] D. Bassett, P.D. Currie, Identification of a zebrafish model of muscular dystrophy, Clin. Exp. Pharmacol. Physiol. 31 (2004) 537–540.
[31] V. Cenni, P. Sabatelli, E. Mattioli, S. Marmiroli, C. Capanni, et al., Lamin A N-terminal phosphorylation is associated with myoblast activation: impairment in Emery-Dreifuss muscular dystrophy, J. Med. Genet. 42 (2005) 214–220.
[32] A. Nicolli, E. Basso, V. Petronilli, R.M. Wenger, P. Bernardi, Interactions of cyclophilin with the mitochondrial inner membrane and regulation of the permeability transition pore, a cyclosporin A-sensitive channel, J. Biol. Chem. 271 (1996) 2185–2192.
[33] M. Wu, A. Neilson, A.L. Swift, R. Moran, J. Tamagnine, et al., Multiparameter metabolic analysis reveals a close link between attenuated mitochondrial bioenergetic function and enhanced glycolysis dependency in human tumor cells, Am. J. Physiol. Cell Physiol. 292 (2007) C125–C136.
[34] J. Berger, T. Sztal, P.D. Currie, Quantification of birefringence readily measures the level of muscle damage in zebrafish, Biochem. Biophys. Res. Commun. 423 (2012) 785–788.
[35] A. Merlini, T. Angelin, P. Tiepolo, P. Braghetta, et al., Cyclosporin A corrects mitochondrial dysfunction and muscle apoptosis in patients with collagen VI myopathies, Proc. Natl. Acad. Sci. U. S. A. 105 (2008) 5225–5229.
[36] A. Angelin, P. Bonaldo, P. Bernardi, Altered threshold of the mitochondrial permeability transition pore in Ullrich congenital muscular dystrophy, Biochim. Biophys. Acta 1777 (2008) 893–896.
[37] C. Pellegrini, A. Zulian, F. Gualandi, E. Manzati, L. Merlini, et al., Melanocytes-A novel tool to study mitochondrial dysfunction in Duchenne muscular dystrophy, J. Cell Physiol. 228 (2013) 1323–1331.
[38] D.I. Bassett, P.D. Currie, The zebrafish as a model for muscular dystrophy and congenital myopathy, Hum. Mol. Genet. 12 (Spec No 2) (2003) R265–R270.
[39] D.I. Bassett, R.J. Bryson-Richardson, D.F. Daggett, P. Gautier, D.G. Keenan, et al., Dystrophin is required for the formation of stable muscle attachments in the zebrafish embryo, Development 130 (2003) 5851–5860.
[40] V. Ljubicic, M. Burt, B.J. Jasmin, The therapeutic potential of skeletal muscle plasticity in Duchenne muscular dystrophy: phenotypic modifiers as pharmacologic targets, FASEB J. 28 (2014) 548–568.
[41] J.V. Chakkalakal, M.A. Harrison, S. Carbonetto, E. Chin, R.N. Michel, et al., Stimulation of calcineurin signaling attenuates the dystrophic pathology in *mdx* mice, Hum. Mol. Genet. 13 (2004) 379–388.
[42] N. Stupka, D.R. Plant, J.D. Schertzer, T.M. Emerson, R. Bassel-Duby, et al., Activated calcineurin ameliorates contraction-induced injury to skeletal muscles of *mdx* dystrophic mice, J. Physiol. 575 (2006) 645–656.
[43] J.T. Seto, K.G. Quinlan, M. Lek, X.F. Zheng, F. Garton, et al., ACTN3 genotype influences muscle performance through the regulation of calcineurin signaling, J. Clin. Invest. 123 (2013) 4255–4263.
[44] M.W. Hogarth, P.J. Houweling, K.C. Thomas, H. Gordish-Dressman, L. Bello, et al., Evidence for ACTN3 as a genetic modifier of Duchenne muscular dystrophy, Nat. Commun. 8 (2017) 14143.
[45] K. Wrogemann, M.C. Blanchaer, Oxidative phosphorylation by muscle mitochondria of dystrophic mice, Can. J. Biochem. 45 (1967) 1271–1278.
[46] K. Wrogemann, M.C. Blanchaer, Respiration and oxidative phosphorylation by muscle and heart mitochondria of hamsters with hereditary myocardiopathy and polymyopathy, Can. J. Biochem. 46 (1968) 323–329.
[47] K. Wrogemann, M.C. Blanchaer, B.E. Jacobson, A calcium-associated magnesium-responsive defect of respiration and oxidative phosphorylation by skeletal muscle mitochondria of BIO 14.6 dystrophic hamsters, Life Sci. II (9) (1970) 1167–1173.
[48] V. Robert, M.L. Massimino, V. Tosello, R. Marsault, M. Cantini, et al., Alteration in calcium handling at the subcellular level in *mdx* myotubes, J. Biol. Chem. 276 (2001) 4647–4651.
[49] K. Wrogemann, B.E. Jacobson, M.C. Blanchaer, On the mechanism of a calcium-associated defect of oxidative phosphorylation in progessive muscular dystrophy, Arch. Biochem. Biophys. 159 (1973) 267–278.
[50] D.P. Millay, S.A. Goonasekera, M.A. Sargent, M. Maillet, B.J. Aronow, et al., Calcium influx is sufficient to induce muscular dystrophy through a TRPC-dependent mechanism, Proc. Natl. Acad. Sci. U. S. A. 106 (2009) 19023–19028.
[51] S.A. Goonasekera, C.K. Lam, D.P. Millay, M.A. Sargent, R.J. Hajjar, et al., Mitigation of muscular dystrophy in mice by SERCA overexpression in skeletal muscle, J. Clin. Invest. 121 (2011) 1044–1052.

[52] S.A. Goonasekera, J. Davis, J.Q. Kwong, F. Accornero, L. Wei-Lapierre, et al., Enhanced Ca^{2+} influx from STIM1-Orai1 induces muscle pathology in mouse models of muscular dystrophy, Hum. Mol. Genet. 23 (2014) 3706–3715.
[53] A.R. Burr, D.P. Millay, S.A. Goonasekera, K.H. Park, M.A. Sargent, et al., Na^{+} dysregulation coupled with Ca^{2+} entry through NCX1 promotes muscular dystrophy in mice, Mol. Cell Biol. 34 (2014) 1991–2002.
[54] R. Ramadasan-Nair, N. Gayathri, S. Mishra, B. Sunitha, R.B. Mythri, et al., Mitochondrial alterations and oxidative stress in an acute transient mouse model of muscle degeneration: implications for muscular dystrophy and related muscle pathologies, J. Biol. Chem. 289 (2014) 485–509.
[55] R. Rizzuto, M. Brini, M. Murgia, T. Pozzan, Microdomains with high Ca^{2+} close to IP3-sensitive channels that are sensed by neighboring mitochondria, Science 262 (1993) 744–747.
[56] C. Cardenas, R.A. Miller, I. Smith, T. Bui, J. Molgo, et al., Essential regulation of cell bioenergetics by constitutive InsP3 receptor Ca^{2+} transfer to mitochondria, Cell 142 (2010) 270–283.
[57] R. Rizzuto, D. De Stefani, A. Raffaello, C. Mammucari, Mitochondria as sensors and regulators of calcium signalling, Nat. Rev. Mol. Cell Biol. 13 (2012) 566–578.
[58] V. Eisner, G. Csordas, G. Hajnoczky, Interactions between sarco-endoplasmic reticulum and mitochondria in cardiac and skeletal muscle – pivotal roles in Ca^{2+} and reactive oxygen species signaling, J. Cell Sci. 126 (2013) 2965–2978.
[59] D.M. Booth, B. Enyedi, M. Geiszt, P. Varnai, G. Hajnoczky, Redox nanodomains are induced by and control calcium signaling at the ER-mitochondrial interface, Mol. Cell 63 (2016) 240–248.
[60] A. Espinosa, C. Henriquez-Olguin, E. Jaimovich, Reactive oxygen species and calcium signals in skeletal muscle: a crosstalk involved in both normal signaling and disease, Cell Calcium 60 (2016) 172–179.
[61] P. Gailly, B. Boland, B. Himpens, R. Casteels, J.M. Gillis, Critical evaluation of cytosolic calcium determination in resting muscle fibres from normal and dystrophic (mdx) mice, Cell Calcium 14 (1993) 473–483.
[62] D.B. Zorov, M. Juhaszova, S.J. Sollott, Mitochondrial reactive oxygen species (ROS) and ROS-induced ROS release, Physiol. Rev. 94 (2014) 909–950.
[63] C. De Palma, E. Clementi, Nitric oxide in myogenesis and therapeutic muscle repair, Mol. Neurobiol. 46 (2012) 682–692.
[64] C. De Palma, F. Morisi, S. Pambianco, E. Assi, T. Touvier, et al., Deficient nitric oxide signalling impairs skeletal muscle growth and performance: involvement of mitochondrial dysregulation, Skelet. Muscle 4 (2014) 22.
[65] F. Di Lisa, R. Menabò, M. Canton, M. Barile, P. Bernardi, Opening of the mitochondrial permeability transition pore causes depletion of mitochondrial and cytosolic NAD^{+} and is a causative event in the death of myocytes in postischemic reperfusion of the heart, J. Biol. Chem. 276 (2001) 2571–2575.
[66] A. Vinogradov, A. Scarpa, B. Chance, Calcium and pyridine nucleotide interaction in mitochondrial membranes, Arch. Biochem. Biophys. 152 (1972) 646–654.
[67] C. Scott Boyer, G.A. Moore, P. Moldeus, Submitochondrial localization of the NAD^{+} glycohydrolase. Implications for the role of pyridine nucleotide hydrolysis in mitochondrial calcium fluxes, J. Biol. Chem. 268 (1993) 4016–4020.
[68] L.R. Stein, S. Imai, The dynamic regulation of NAD metabolism in mitochondria, Trends Endocrinol. Metab. 23 (2012) 420–428.
[69] C. Dölle, J.G. Rack, M. Ziegler, NAD and AP-ribose metabolism in mitochondria, FEBS J. 280 (2013) 3530–3541.
[70] M. Barile, S. Passarella, G. Danese, E. Quagliariello, Rat liver mitochondria can synthesize nicotinamide adenine dinucleotide from nicotinamide mononucleotide and ATP via a putative matrix nicotinamide mononucleotide adenylyltransferase, Biochem. Mol. Biol. Int. 38 (1996) 297–306.
[71] P.C. Even, A. Decrouy, A. Chinet, Defective regulation of energy metabolism in *mdx*-mouse skeletal muscles, Biochem. J. 304 (1994) 649–654.
[72] A.V. Kuznetsov, K. Winkler, F.R. Wiedemann, P. von Bossanyi, K. Dietzmann, et al., Impaired mitochondrial oxidative phosphorylation in skeletal muscle of the dystrophin-deficient mdx mouse, Mol. Cell Biochem. 183 (1998) 87–96.
[73] M. Onopiuk, W. Brutkowski, K. Wierzbicka, S. Wojciechowska, J. Szczepanowska, et al., Mutation in dystrophin-encoding gene affects energy metabolism in mouse myoblasts, Biochem. Biophys. Res. Commun. 386 (2009) 463–466.
[74] E. Rybalka, C.A. Timpani, M.B. Cooke, A.D. Williams, A. Hayes, Defects in mitochondrial ATP synthesis in dystrophin-deficient *mdx* skeletal muscles may be caused by complex I insufficiency, PLoS One 9 (2014) e115763.
[75] L. Azzolin, E. Basso, F. Argenton, P. Bernardi, Mitochondrial Ca^{2+} transport and permeability transition in zebrafish (Danio rerio), Biochim. Biophys. Acta 1797 (2010) 1775–1779.
[76] P.R. Sweeny, Ultrastructure of the developing myotendinous junction of genetic dystrophic chickens, Muscle Nerve 6 (1983) 207–217.
[77] J.G. Tidball, D.J. Law, Dystrophin is required for normal thin filament-membrane associations at myotendinous junctions, Am. J. Pathol. 138 (1991) 17–21.
[78] D.J. Law, J.G. Tidball, Dystrophin deficiency is associated with myotendinous junction defects in prenecrotic and fully regenerated skeletal muscle, Am. J. Pathol. 142 (1993) 1513–1523.
[79] J.C. Ridge, J.G. Tidball, K. Ahl, D.J. Law, W.L. Rickoll, Modifications in myotendinous junction surface morphology in dystrophin-deficient mouse muscle, Exp. Mol. Pathol. 61 (1994) 58–68.
[80] S.A. Parsons, B.J. Wilkins, O.F. Bueno, J.D. Molkentin, Altered skeletal muscle phenotypes in calcineurin Aα and Aβ gene-targeted mice, Mol. Cell. Biol. 23 (2003) 4331.
[81] S.A. Parsons, D.P. Millay, B.J. Wilkins, O.F. Bueno, G.L. Tsika, et al., Genetic loss of calcineurin blocks mechanical overload-induced skeletal muscle fiber type switching but not hypertrophy, J. Biol. Chem. 279 (2004) 26192–26200.
[82] O.M. Dorchies, J. Reutenauer-Patte, E. Dahmane, H.M. Ismail, O. Petermann, et al., The anticancer drug tamoxifen counteracts the pathology in a mouse model of duchenne muscular dystrophy, Am. J. Pathol. 182 (2013) 485–504.
[83] K.R. Sharma, M.A. Mynhier, R.G. Miller, Cyclosporine increases muscular force generation in Duchenne muscular dystrophy, Neurology 43 (1993) 527–532.
[84] R.G. Miller, K.R. Sharma, G.K. Pavlath, E. Gussoni, M. Mynhier, et al., Myoblast implantation in Duchenne muscular dystrophy: the San Francisco study, Muscle Nerve 20 (1997) 469–478.
[85] J. Kirschner, J. Schessl, U. Schara, B. Reitter, G.M. Stettner, et al., Treatment of Duchenne muscular dystrophy with ciclosporin A: a randomised, double-blind, placebo-controlled multicentre trial, Lancet Neurol. 9 (2010) 1053–1059.
[86] G. Fischer, B. Wittmann-Liebold, K. Lang, T. Kiefhaber, F.X. Schmid, Cyclophilin and peptidyl-prolyl *cis-trans* isomerase are probably identical proteins, Nature 337 (1989) 476–478.
[87] J.C. Shing, R.J. Bram, Yet another hump for CAML: support of cell survival independent of tail-anchored protein insertion, Cell. Death. Dis. 8 (2017) e2960.
[88] A.M. Blain, V.W. Straub, δ-Sarcoglycan-deficient muscular dystrophy: from discovery to therapeutic approaches, Skelet. Muscle 1 (2011) 13.
[89] P. Bonaldo, P. Braghetta, M. Zanetti, S. Piccolo, D. Volpin, et al., Collagen VI deficiency induces early onset myopathy in the mouse: an animal model for Bethlem myopathy, Hum. Mol. Genet. 7 (1998) 2135–2140.
[90] R. Buti, J.H. Flisiak, W.L. Kao, et al., Alisporivir with peginterferon/ribavirin in patients with chronic hepatitis C genotype 1 infection who failed to respond to or relapsed after prior interferon-based therapy: FUNDAMENTAL, a Phase II trial, J. Viral Hepat. 22 (2015) 596–606.
[91] S. Zeuzem, R. Flisiak, J.M. Vierling, W. Mazur, G. Mazzella, et al., Randomised clinical trial: alisporivir combined with peginterferon and ribavirin in treatment-naive patients with chronic HCV genotype 1 infection (ESSENTIAL II), Aliment. Pharmacol. Ther. 42 (2015) 829–844.